Journal of Applied Mathematics and Physics, 2022, 10, 2232-2244
https://www.scirp.org/journal/jamp
ISSN Online: 2327-4379
ISSN Print: 2327-4352

Theoretical Study on the Effect of Multiband Structure on Critical Temperature and Electronic Specific Heat in SmOFeAs Iron Pnictide Superconductor

Shamin Masih*, Piyush Masih, Sarita Khandka

SHUATS, Prayagraj, India
Email: *shamin.masih@shiats.edu.in, piyush.masih@shiats.edu.in, sarita.khandka@shiats.edu.in

How to cite this paper: Masih, S., Masih, P. and Khandka, S. (2022) Theoretical Study on the Effect of Multiband Structure on Critical Temperature and Electronic Specific Heat in SmOFeAs Iron Pnictide Superconductor. *Journal of Applied Mathematics and Physics*, **10**, 2232-2244.
https://doi.org/10.4236/jamp.2022.107153

Received: June 24, 2022
Accepted: July 23, 2022
Published: July 26, 2022

Abstract

In the present theoretical work, superconducting order parameter (Δ) and electronic specific heat (C_{es}) of SmOFeAs iron pnictide (IP) superconductor has been studied using multiband (MB) model of IP superconductors. Attempt has been made to use the MB structure of IP superconductors and expressions for critical temperature (T_c) and C_{es} are obtained, calculations being made for one, two and three bands of SmOFeAs. It has been found that MB results are close to the experimental value of T_c for this compound. C_{es} calculations show jump of 1.5×10^{-5} eV/atom K, 4×10^{-5} eV/atom K and 4×10^{-5} eV/atom K for one, two and three band models respectively. The study brings out the importance of MB structure in IPs, highlighting the fact that increasing the number of bands, increases T_c. The specific heat jump (ΔC) does not correspond to the BCS value, thereby proving that IPs are unconventional in nature.

Keywords

Electronic Specific Heat, Iron Pnictide Superconductor, Multiband, Superconducting Order Parameter

1. Introduction

The year 2006 [1] witnessed a major breakthrough in the field of superconductivity with the discovery of a new class of iron based superconductors called IPs. Further increase in T_c in the same class of SCs was witnessed in the year 2008 [2]. Researchers all over the world were amused at the discovery made by Hideo Hosono [3] and coworkers in the course of exploration of magnetic semicon-

ductors. These transition metal based superconductors having general formula LnOFeAs (Ln = La, Ce, Sm, Gd, Nd, Pr) are layered structures with alternate LnO & FeAs layers, superconductivity believed to be present because of the FeAs layers. The structure orientation of Fe atoms shows it to be surrounded by four arsenic atoms resulting in a distorted tetrahedral geometry. The iron atoms are seen to make a square lattice and arsenic atoms are placed at the centre of each square being displaced above & below the Fe planes. IPs are second in class after the cuprates [4] to have high T_c of around 55 Kas shown by experimental studies of Ren and Chen [5] [6] and theoretical study by Mebrahtu [7]. Interest in this newly class of discovered materials was generated not only because of its high T_c, but also because iron, being the most magnetic material [8] that could have been destructive for superconductivity, showed high values of T_c. Within a span of ten years, the quantum of research in this field is high because of the extraordinary properties exhibited by these compounds. It has been shown that in the normal state, these compounds are semi-metals [9] (upon doping [10] or application of pressure [11] [12] [13] [14] is seen to increase T_c in IPs). Several experimentation in this field is trying to study minutely various properties associated with them. Angle resolved photoemission experiments [15] have demonstrated that IPs are MB [16] [17] in nature. Iron has five bands at the Fermi surface and all the five d-bands of iron are relevant in studying the superconducting properties of these compounds as opposed to the single band of cuprates [18] [19] and BCS [20] superconductors or the two band MgB_2 [21] [22] [23]. Previous theories have found that MB nature [24] of IPs makes them a significant class in the vast area of superconductivity and that MB structure serves as an important ingredient for high T_c [25] for this class of compounds. The four unpaired d electrons of iron are seen to hybridise [26] with the three unpaired p electrons of arsenic, resulting in bands found at the Fermi surface due to overlapping orbitals [27] [28]. Raghu *et al.* has discussed that a minimal two band model [29] is needed for the superconducting IPs. Several others have also studied two bandsuperconductivity [30] [31] [32] [33]. Three band superconductivities [34] have also been studied using different theories like Eliashberg theory [35], Ginzburg Landau theory [36], etc.

Over the years, the MB property of IPs is exploited in understanding these materials in a better way. Earlier, also it has been found that interband interactions lead to higher T_c in cuprate SCs [37]. Since IPs are also MB SCs with nesting present at the Fermi surface, therefore it is desirable to investigate the role of interband and intraband interactions on various superconducting properties. Several properties of IPs are investigated to understand the mechanism of this special class of high temperature superconductors (HTS). The electronic specific heat of IPs is studied using electron-Cooper pair interaction by Mukubwa [38]. Mohamed *et al.* have explained pressure effect for HTS using pressure dependent Schrodinger equation and string theory [39]. With this motivation in mind, T_c and C_{es} of SmOFeAs compound [40] [41] [42] [43] is investigated using a MB

model, employing Green's function technique and the results are compared with experimental values.

2. Mathematical Technique and Formulation

In the present theoretical work, the two thermodynamical properties which is Δ and C_{es} of SmOFeAs are investigated as a function of the number of bands. The model Hamiltonian uses itinerant nature of electrons. It is described as:

$$H = \sum_{mk\sigma} E_{mk\sigma} C^{+}_{mk\sigma} C_{mk\sigma} - \sum_{mkk'} V_{mm} C^{+}_{mk\uparrow} C^{+}_{m-k\downarrow} C_{m-k'\downarrow} C_{mk'\uparrow} - V_{mn} \sum_{\substack{kk' \\ m\neq n}} C^{+}_{mk\uparrow} C^{+}_{m-k\downarrow} C_{n-k'\downarrow} C_{nk'\uparrow} \tag{1}$$

In Equation (1), the first term represents energy of itinerant electrons. The second term denotes the intraband interaction term. V_{mm} is the intraband interaction potential. The third term is the interband interaction term. It represents tunnelling between the bands. V_{mn} is the interband interaction potential. m, n is band index, k is wave vector and σ is spin index for fermions.

Considering the two Green's functions

$$G_{\substack{\uparrow\uparrow \\ r\,s\,q\,q}} = \left\langle\left\langle C_{rq\uparrow}, C^{+}_{sq\uparrow}\right\rangle\right\rangle \tag{2a}$$

$$G_{\substack{\downarrow\uparrow \\ rs-qq}} = \left\langle\left\langle C^{+}_{r-q\downarrow}, C^{+}_{sq\uparrow}\right\rangle\right\rangle \tag{2b}$$

Here r and s are the band index and q denotes wave vector.

Using the first Green function (2a), the equation of motion is expressed as:

$$\left(\omega - E_{rq\uparrow}\right) G_{\substack{\uparrow\uparrow \\ r\,s\,q\,q}} = \frac{1}{2\pi}\delta_{rs} - V_{rr}\Delta_{rr} G_{\substack{\downarrow\uparrow \\ r\,s-qq}} - \sum_{\substack{n \\ r\neq n}} V_{rn}\gamma_{\downarrow\downarrow} G_{\substack{\uparrow\uparrow \\ n\,sqq}} - \sum_{\substack{n \\ r\neq n}} V_{rn}\Delta_{nn} G_{\substack{\downarrow\uparrow \\ r\,s-qq}} \tag{3}$$

Using the second Green function (2b), the second equation of motion is written as:

$$\left(\omega + E_{r-q\downarrow}\right) G_{\substack{\downarrow\uparrow \\ r\,s-qq}} = -V_{rr}\Delta_{rr} G_{\substack{\uparrow\uparrow \\ r\,s\,qq}} - V_{rm}\sum_{\substack{m \\ m\neq r}} \Delta_{mm} G_{\substack{\uparrow\uparrow \\ r\,s\,qq}} + V_{rm}\sum_{\substack{m \\ m\neq r}} \gamma_{\uparrow\uparrow} G_{\substack{\downarrow\uparrow \\ m\,s-qq}} \tag{4}$$

where the OPs are defined as:

$$\Delta_{rr} = \sum_{k'} \left\langle C_{r-k'\downarrow}, C_{rk'\uparrow}\right\rangle$$

$$\Delta_{nn} = \sum_{k'} \left\langle C_{n-k'\downarrow}, C_{nk'\uparrow}\right\rangle$$

$$\gamma_{\downarrow\downarrow} = \sum_{k'} \left\langle C^{+}_{r-q\downarrow}, C_{n-k'\downarrow}\right\rangle$$

is number factor representing number of charge per unit volume.

2.1. One Band Model (OBM)

Using the two equations of Motion (3) and (4) and substituting $r = s = 1$, calculations are done for OBM using $E_{1q\uparrow} = E_{1-q\downarrow}$ and $G_1 = G_{\substack{\uparrow\uparrow \\ 11q\,q}}$ and $G_2 = G_{\substack{\downarrow\uparrow \\ 11-q\,q}}$

Δ is defined as:

$$\Delta_{11} = \sum_K V_{11} \left\langle C_{1k\uparrow}^{+}, C_{1-k\downarrow}^{+} \right\rangle \tag{5}$$

The correlation function (CF) $\left\langle C_{1k\uparrow}^{+}, C_{1-k\downarrow}^{+} \right\rangle$ is related to G_2 as:

$$\left\langle C_{1k\uparrow}^{+}, C_{1-k\downarrow}^{+} \right\rangle = -\frac{1}{i} \int_{-\infty}^{\infty} \frac{G_2(\omega + i\varepsilon) - G_2(\omega - i\varepsilon)}{e^{\frac{\omega}{kT}} - \eta} \tag{6}$$

where, $\eta = -1$ for fermions, k is Boltzmann constant and T is absolute temperature in kelvin.

The expression of Δ is obtained as:

$$\Delta_{11} = \frac{V_{11}^2 \Delta_{11}}{2\sqrt{E_{1q\uparrow}^2 + (V_{11}\Delta_{11})^2}} \tanh \frac{\sqrt{E_{1q\uparrow}^2 + (V_{11}\Delta_{11})^2}}{2kT} \tag{7}$$

Converting summation into integration with cut off energy $\pm\hbar\omega_D$ from the Fermi level and substituting $T \to T_C$ as $\Delta \to 0$:

$$1 = N_0 \int_0^{\hbar\omega_D} \frac{V_{11}}{2E_{1q\uparrow}} \tanh \frac{E_{1q\uparrow}}{2kT_C} dE_{1q\uparrow} \tag{8}$$

T_c can be expressed as:

$$1 = N_O V_{11} \int_0^{\hbar\omega_D} \frac{1}{2\sqrt{E_{1q\uparrow}^2 + \overline{\Delta}_{11}^2}} \tanh \frac{\sqrt{E_{1q\uparrow}^2 + \overline{\Delta}_{11}^2}}{2kT} dE_{1q\uparrow} \tag{9}$$

Here $\overline{\Delta}_{11} = V_{11}\Delta_{11}$

For OBM, C_{es} is defined as:

$$C_{es}^1 = \frac{\partial}{\partial T} \frac{1}{N} \sum 2E_{1q\uparrow} \left\langle c_{1k\uparrow}^{+}, c_{1k\uparrow} \right\rangle \tag{10}$$

CF $\left\langle C_{1k\uparrow}^{+}, C_{1k\uparrow} \right\rangle$ is related to G_1 as:

$$\left\langle C_{1k\uparrow}^{+}, C_{1k\uparrow} \right\rangle = \frac{-1}{i} \int_{-\infty}^{\infty} \frac{G_1(\omega + iE) - G_1(\omega - iE)}{e^{\frac{\omega}{kT}} - \eta} \tag{11}$$

C_{es} for OBM comes out as:

$$C_{es}^1 = \frac{1}{2NkT^2} \sum E_{1q\uparrow}^2 \operatorname{sech}^2 \left(\frac{\sqrt{E_{1q\uparrow}^2 + (V_{11}\Delta_{11})^2}}{2kT} \right) \tag{12}$$

Converting summation into integration,

$$C_{es}^1 = \frac{1}{NkT^2} \int_0^{\hbar\omega_D} E_{1q\uparrow}^2 \operatorname{sech}^2 \left(\frac{\sqrt{E_{1q\uparrow}^2 + (V_{11}\Delta_{11})^2}}{2kT} \right) \tag{13}$$

2.2. Two Band Model (TBM)

Using the two equations of Motion (3) and (4) and substituting the four conditions: $r = 1$, $s = 1$; $r = 1$, $s = 2$; $r = 2$, $s = 2$ and $r = 2$, $s = 1$, calculations are done

for TBM using $G_1 = G_{\uparrow\uparrow}$, $G_2 = G_{\downarrow\uparrow}$, $G_3 = G_{12qq}^{\uparrow\uparrow}$, $G_4 = G_{12-qq}^{\downarrow\uparrow}$, $G_5 = G_{22qq}^{\uparrow\uparrow}$, $G_6 = G_{22-qq}^{\downarrow\uparrow}$, $E_{1q\uparrow} = E_{1-q\downarrow}^{11qq}$ and $E_{2q\uparrow} = E_{2-q\downarrow}^{11-qq}$

Similarly for TBM, the following results are obtained:

$$\left\langle C_{1k\uparrow}^{+}, C_{1-k\downarrow}^{+} \right\rangle = \frac{V_{11}\Delta_{11} + V_{12}\Delta_{22}}{2\sqrt{E_{1q\uparrow}^2 + \left(V_{11}\Delta_{11} + V_{12}\Delta_{22}\right)^2}} \tanh \frac{\sqrt{E_{1q\uparrow}^2 + \left(V_{11}\Delta_{11} + V_{12}\Delta_{22}\right)^2}}{2kT} \tag{14}$$

The second CF is obtained as:

$$\left\langle C_{2k\uparrow}^{+}, C_{2-k\downarrow}^{+} \right\rangle = \frac{V_{21}\Delta_{11} + V_{22}\Delta_{22}}{2\sqrt{E_{2q\uparrow}^2 + \left(V_{21}\Delta_{11} + V_{22}\Delta_{22}\right)^2}} \tanh \frac{\sqrt{E_{2q\uparrow}^2 + \left(V_{21}\Delta_{11} + V_{22}\Delta_{22}\right)^2}}{2kT} \tag{15}$$

C_{es}^{21} comes out as:

$$C_{es}^{21} = \frac{1}{2NkT^2\Delta_1\Delta_2} \sum E_{1q\uparrow}^2 \operatorname{sech}^2 \left(\frac{\sqrt{E_{1q\uparrow}^2 + \Delta_1^2}}{2kT} \right) \tag{16}$$

Converting summation into integration,

$$C_{es}^{21} = \frac{1}{NkT^2\Delta_1\Delta_2} \int_0^{\hbar\omega_D} E_{1q\uparrow}^2 \operatorname{sech}^2 \left(\frac{\sqrt{E_{1q\uparrow}^2 + \Delta_1^2}}{2kT} \right) \tag{17}$$

C_{es} for the second band corresponding to G_5 is defined as:

$$C_{es}^{22} = \frac{\partial}{\partial T} \frac{1}{N} \sum 2E_{2q\uparrow} \left\langle c_{2k\uparrow}^{+}, c_{2k\uparrow} \right\rangle \tag{18}$$

CF $\left\langle C_{2k\uparrow}^{+}, C_{2k\uparrow} \right\rangle$ is related to G_5 as:

$$\left\langle C_{2k\uparrow}^{+}, C_{2k} \right\rangle = \frac{\frac{-1}{i} \int_{-\infty}^{\infty} G_5\left(\omega + iE\right) - G_5\left(\omega - iE\right)}{e^{\frac{\omega}{kT}} - \eta} \tag{19}$$

C_{es}^{22} is calculated as:

$$C_{es}^{22} = \frac{1}{2NkT^2} \sum E_{2q\uparrow}^2 \operatorname{sech}^2 \left(\frac{\sqrt{E_{2q\uparrow}^2 + \Delta_2^2}}{2kT} \right) \tag{20}$$

Converting summation into integration,

$$C_{es}^{22} = \frac{1}{NkT^2} \int_0^{\hbar\omega_D} E_{2q\uparrow}^2 \operatorname{sech}^2 \left(\frac{\sqrt{E_{2q\uparrow}^2 + \Delta_2^2}}{2kT} \right) \tag{21}$$

2.3. Three Band Model (THBM)

Using the two equations of Motion (3) and (4) and substituting the following eight conditions,

$r = 1$, $s = 1$; $r = 1$, $s = 2$; $r = 1$, $s = 3$; $r = 2$, $s = 1$; $r = 2$, $s = 2$; $r = 2$, $s = 3$; $r = 3$, $s = 1$; $r = 3$, $s = 2$ and $r = 3$, $s = 3$, using the ten Green's functions G_1 to G_{10} and

making following substitutions:

$$E_{1q\uparrow} = E_{1-q\downarrow}, E_{21q\uparrow} = E_{2-q\downarrow}, E_{3q\uparrow} = E_{3-q\downarrow}$$

For the first band,

$$\left\langle C_{1k\uparrow}^{+}, C_{1-k\downarrow}^{+} \right\rangle = \frac{V_{11}\Delta_{11} + V_{12}\Delta_{22} + V_{13}\Delta_{33}}{2\sqrt{\Delta_1^2 + \left(E_{1q\uparrow} + \frac{V_{12}V_{31}}{V_{32}}\gamma_{\uparrow\uparrow}\right)^2}} \tanh \frac{\sqrt{\Delta_1^2 + \left(E_{1q\uparrow} + \frac{V_{12}V_{31}}{V_{32}}\gamma_{\uparrow\uparrow}\right)^2}}{2kT} \tag{22}$$

For the second band, Δ is obtained as:

$$\Delta_{22} = \frac{V_{21}\Delta_{11} + V_{22}\Delta_{22} + V_{23}\Delta_{33}}{2\sqrt{E_{2q\uparrow}^2 + \left(V_{21}\Delta_{11} + V_{22}\Delta_{22} + V_{23}\Delta_{33}\right)^2}} \times \tanh \frac{\sqrt{E_{2q\uparrow}^2 + \left(V_{21}\Delta_{11} + V_{22}\Delta_{22} + V_{23}\Delta_{33}\right)^2}}{2kT} \tag{23}$$

For the third band, CF related to G_{10} is written as:

$$\left\langle C_{3k\uparrow}^{+}, C_{3-k\downarrow}^{+} \right\rangle = -\frac{1}{i}\int_{-\infty}^{\infty} \frac{G_{10}\left(\omega + i\varepsilon\right) - G_{10}\left(\omega - i\varepsilon\right)}{e^{\frac{\omega}{KT}} - \eta} \tag{24}$$

The corresponding $\Delta_{33} = V_{33}\left\langle C_{3k\uparrow}^{+}, C_{3-k\downarrow}^{+} \right\rangle$ comes out to be:

$$\Delta_{33} = \frac{V_{31}\Delta_{11} + V_{32}\Delta_{22} + V_{33}\Delta_{33}}{2\sqrt{\left(V_{31}\Delta_{11} + V_{32}\Delta_{22} + V_{33}\Delta_{33}\right)^2 + \left(E_{3q\uparrow} + \frac{V_{32}V_{13}}{V_{12}}\gamma_{\uparrow\uparrow}\right)^2}} \times \tanh \frac{\sqrt{\left(V_{31}\Delta_{11} + V_{32}\Delta_{22} + V_{33}\Delta_{33}\right)^2 + \left(E_{1q\uparrow} + \frac{V_{32}V_{13}}{V_{12}}\gamma_{\uparrow\uparrow}\right)^2}}{2kT} \tag{25}$$

For THBM, expression for C_{es}^{31} is:

$$C_{es}^{31} = \frac{1}{2NkT^2}\sum E_{1q\uparrow}\left(E_{1q\uparrow} + \frac{V_{12}V_{31}}{V_{32}}\gamma\right)\operatorname{sech}^2\left(\frac{\sqrt{\left(E_{1q\uparrow} + \frac{V_{12}V_{31}}{V_{32}}\gamma\right)^2 + \Delta_1^2}}{2KT}\right) \tag{26}$$

Converting summation into integration gives:

$$C_{es}^{31} = \int_0^{\hbar\omega_D} \frac{1}{NkT^2} E_{1q\uparrow}\left(E_{1q\uparrow} + \frac{V_{12}V_{31}}{V_{32}}\gamma\right)\operatorname{sech}^2\left(\frac{\sqrt{\left(E_{1q\uparrow} + \frac{V_{12}V_{31}}{V_{32}}\gamma\right)^2 + \Delta_1^2}}{2KT}\right) \tag{27}$$

C_{es}^{32} is calculated as:

$$C_{es}^{32} = \frac{1}{2NkT^2}\sum E_{2q\uparrow}^2 \operatorname{sech}^2\left(\frac{\sqrt{E_{2q\uparrow}+\Delta_2^2}}{2kT}\right) \tag{28}$$

Converting summation into integration,

$$C_{es}^{32} = \frac{1}{NkT^2}\int_0^{\hbar\omega_D} E_{2q\uparrow}^2 \operatorname{sech}^2\left(\frac{\sqrt{E_{2q\uparrow}+\Delta_2^2}}{2kT}\right) \tag{29}$$

C_{es} for the third band corresponding to G_9 is:

$$C_{es}^{33} = \frac{\partial}{\partial T}\frac{1}{N}\sum 2E_{3q\uparrow}\left\langle c_{3k\uparrow}^{+}, c_{3k\uparrow}\right\rangle \tag{30}$$

$$C_{es}^{33} = \frac{1}{2NkT^2}\sum E_{3q\uparrow}\sqrt{\xi^2-\Delta_3^2}\operatorname{sech}^2\frac{\sqrt{\left(E_{3q\uparrow}+\frac{V_{32}V_{13}}{V_{12}}\gamma\right)^2+\Delta_3^2}}{2kT} \tag{31}$$

Converting summation into integration,

$$C_{es}^{33} = \frac{1}{NkT^2}\int_0^{\hbar\omega_D} E_{3q\uparrow}\left(E_{3q\uparrow}+\frac{V_{32}V_{13}}{V_{12}}\gamma\right)\operatorname{sech}^2\frac{\sqrt{\left(E_{3q\uparrow}+\frac{V_{32}V_{13}}{V_{12}}\gamma\right)^2+\Delta_3^2}}{2kT} \tag{32}$$

3. Results and Discussion

In this section, the numerical results obtained for T_c and C_{es} of MB SmOFeAs are presented. The results are investigated as a function of the number of bands, expressions being obtained for one, two and three band models, highlighting the MB nature of the superconducting compound.

3.1. Variation of Δ with *T*

Δ is a measure of the binding energy of Cooper pair. Its variation is studied with T as a function of the number of bands.

Figure 1 shows the combined variation of Δ_{11}, Δ_{22} and Δ_{33} with T for OB, TB and THBMs illustrating the rise in T_c with increasing number of bands. It is seen that with increasing T, Δ decreases and at $T = T_c$, Δ = 0. This is the usual behaviour of Δ vs T and hence justified. T_c for OBM comes out to be 11 K; for TBM, T_c is 45 K and for THBM it is 57 K. During calculations, the values of $\hbar\omega_D$ = 0.05 eV, $N = 10^{27}$ eV/atom, $N_o V_{11}$ = 0.24. $N_o V_{12}$ = 0.12, $N_o V_{13}$ = 0.06. The highest value of T_c is seen to be 57 K which is very well in agreement with experimental results [5].

3.2. Variation of C_{es} with *T*

C_{es} is the amount of heat per unit mass required to raise the temperature by one unit. Its variation is studied with T as a function of the number of bands.

Using Equation (13), the variation of C_{es}^{1} with T for OBM shows that initially the SH for SC is less than the SH for normal state (NS), it then suddenly

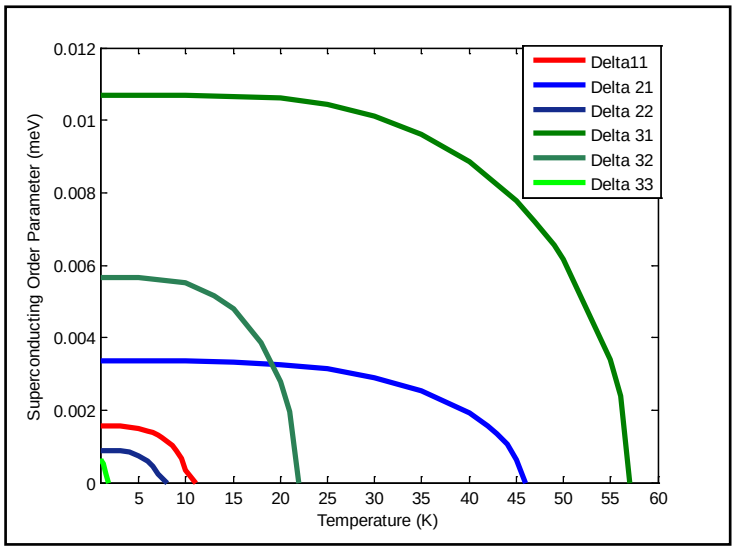

Figure 1. Δ_{11}, Δ_{22} and Δ_{33} (meV) versus T(K) for OB, TB and THBM.

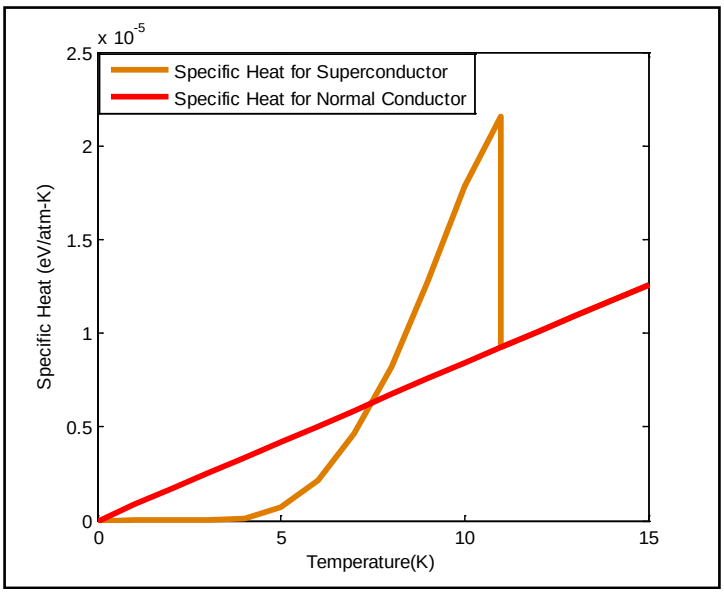

Figure 2. C_{es}^{1} (eV/atom-K) versus T(K) for OBM.

increases and then drags down at a particular T which is the T_c of the system which is 11 K as seen in the **Figure 2**. At T_c, the curve shows a jump ΔC of 1.5 × 10^{-5} eV/atom K which is contrary as seen in the BCS model [44]. $\Delta C/\gamma T_c$ is calculated as 1.101 for the model which is also not in accordance with BCS model [45], thus signifying that IPs are unconventional SCs [46] [47].

Figure 3 shows the combined graph of the variation of C_{es}^{21} and C_{es}^{22} with T for TBM illustrating that initially the SH of SC is less than the SH for NS, it then suddenly increases at 7 K and then drags down atthe T_c for the system, observed at 45 K. ΔC is 4 × 10^{-5} eV/atom K and $\Delta C/\gamma T_c$ is calculated as 0.718 for the model. Both these values are not in accordance with BCS model, thereby showing that IPs are unconventional SCs.

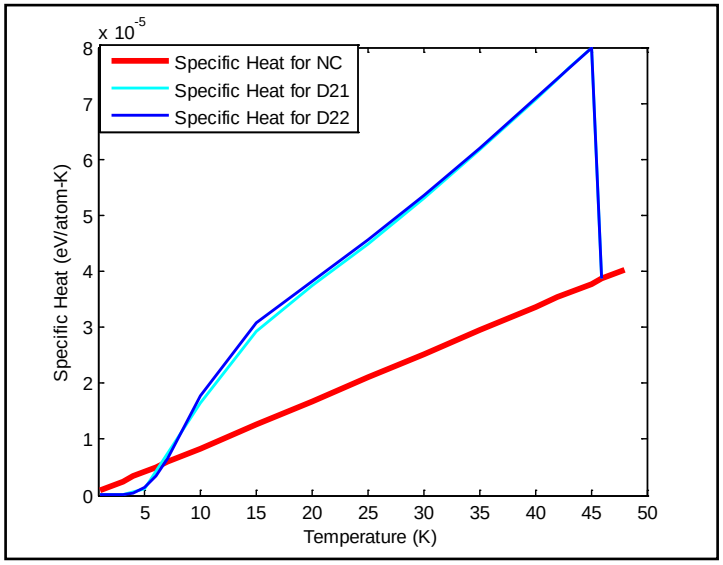

Figure 3. C_{es}^{21} and C_{es}^{22} (eV/atom-K) versus T(K) for TBM.

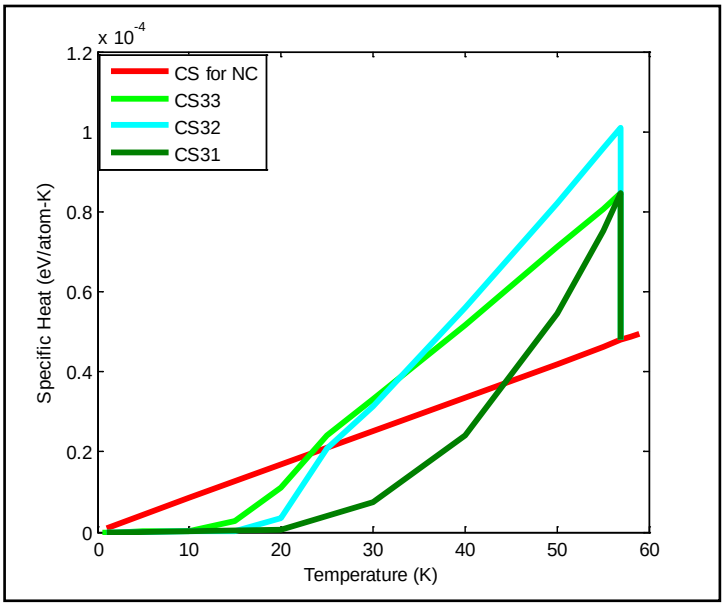

Figure 4. SH C_{es}^{31}, C_{es}^{32} and C_{es}^{33} (eV/atom-K) versus T(K) for THBM.

Figure 4 shows the combined graph of the variation of C_{es}^{31}, C_{es}^{32} and C_{es}^{33} with T for THBM illustrating that initially the SH of SC is less than the SH for NS, it then suddenly increases and then drags down at the T_c for the system observed at 57 K. ΔC is 4×10^{-5} eV/atom K and $\Delta C/\gamma T_c$ is calculated as 0.567 for the model. Both these values are not in accordance with BCS model proving IPs to be unconventional in nature. The value of Sommerfeld coefficientγ for the compound SmOFeAs is 119.4 mJ/mol K^2 [45].

4. Conclusion

The present study has been undertaken to get some information regarding the

behaviour of T_c and electronic specific heat for superconducting SmOFeAs. It is seen that upon increasing the number of bands has shown an increase in T_c which is very well in agreement with experimental results, thereby proving that interband interactions play an important role in enhancing the T_c. Thus this study also supports that MB structures are helpful to stabilize superconductivity and for obtaining high T_c in this class of compounds. This appears reasonable as interband interactions are already found to enhance T_c [25]. The specific heat calculations reveal that IPs are governed by a mechanism other than the BCS one [46]. The sharp peak observed in the specific heat curve is attributed to AFM ordering of Sm^{3+} magnetic ions in the system which is otherwise not seen in the lanthanum compound that has non-magnetic La^{3+} ions [47]. The theoretical model is restricted uptil three bands as suggested by Ummarino [35] that a simple THBM in strong-coupling regime [48] [49] [50] can reproduce in a quantitative way the experimental T_c.

Conflicts of Interest

The authors declare no conflicts of interest regarding the publication of this paper.

References

[1] Kamihara, Y., Hiramatsu, H., Hirano, M., Kawamura, R., Yanagi, H., Kamiya, T. and Hosono, H. (2006) Iron Based Layered Superconductor: LaOFeP. *Journal of American Chemical Society*, **128**, 10012-10013. https://doi.org/10.1021/ja063355c

[2] Kamihara, Y., Watanabe, T., Hirano, M. and Hosono, H. (2008) Iron-Based Layered Superconductor $La[O_{1-x}F_x]FeAs$ (x = 0.05 – 0.12) with T_c = 26 K. *Journal of American Chemical Society*, **130**, 3296-3297. https://doi.org/10.1021/ja800073m

[3] Hosono, H. (2011) Iron Pnictide Superconductors: Discovery and Current Status. *Material Matters*, **4**, 1-9. https://doi.org/10.1007/BF01303701

[4] Bednorz, J.G. and Müller, K.A. (1986) Possible High T_c Superconductivity in the Ba-La-Cu-O System. *Zeilschrift for Physik B*, **64**, 189-193. https://doi.org/10.1209/0295-5075/82/57002

[5] Ren, Z.A., Yang, J., Lu, W., Yi, W., Che, G.C., Dong, X.L., Sun, L.L. and Zhao, Z.X. (2008) Superconductivity in the Iron-Based F-Doped Layered Quaternary Compound $Sm[O_{1-x}F_x]FeAs$. *Europhysics Letters*, **82**, Article ID: 57002. https://doi.org/10.1093/nsr/nwu007

[6] Chen, X., Dai, P., Feng, D., Xiang, T. and Zhang, F.C. (2014) Iron-Based High Transition Temperature Superconductors. *National Science Review*, **1**, 371-395. https://doi.org/10.4236/wjcmp.2015.53016

[7] Mebrahtu, A. and Singh, P. (2015) Coexistence of Superconductivity and Antiferromagnetism in $SmAsO_{1-x}F_xFe$. *World Journal of Condensed Matter Physics*, **5**, 138-147. https://doi.org/10.1063/1.3206093

[8] Day, C. (2009) Iron-Based Superconductors. *Physics Today*, **62**, 36-40. https://doi.org/10.1088/1367-2630/18/12/123003

[9] Tytarenko, A., Nakatsukasa, K., Huang, Y.K., Johnston, S. and Heumen, E.V. (2016) From Bad Metal to Kondo Insulator: Temperature Evolution of the Optical Properties of SmB_6. *New Journal of Physics*, **18**, Article ID: 123003.

[10] Nakajima, M., Ishida, S., Tanaka, T., Kihou, K., Tomioka, Y., Saito, T., Lee, C.H., Fukazawa, H., Kohori, Y., Kakeshita, T., Iyo, A., Ito, T., Eisaki, H. and Uchida, S.I. (2014) Strong Electronic Correlations in Iron Pnictides: Comparison of Optical Spectra for $BaFe_2As_2$-Related Compounds. *Journal of the Physical Society of Japan*, **83**, Article ID: 104703. https://doi.org/10.7566/JPSJ.83.104703

[11] Yi, W., Sun, L., Ren, Z., Lu, W., Dong, X., Zhang, H.J., Dai, X., Fang, Z., Li, Z., Che, G., Yang, J., Shen, X., Zhou, F. and Zhao, Z. (2008) Pressure Effect on Superconductivity of Iron Based Arsenic-Oxide $ReFeAsO_{0.85}$ (Re=Sm and Nd). *Europhysics Letters*, **83**, Article ID: 57002. https://doi.org/10.1209/0295-5075/83/57002

[12] Kobayashi, K., Yamaura, J.I., Iimura, S., Maki, S., Sagayama, H., Kumai, R., Murakami,Y., Takahashi, H., Matsuishi, S. and Hosono, H. (2016) Pressure Effect on Iron-Based Superconductor $LaFeAsO_{1-x}H_x$: Peculiar Response of 1111-Type Structure. *Scientific Reports*, **6**, Article No. 39646. https://doi.org/10.1038/srep39646

[13] Wang, A.F., Xiang, Z.J., Ying, J.J., Yan, Y.J., Cheng, P., Ye, G.J., Luo, X.G. and Chen, X.H. (2012) Pressure Effects on the Superconducting Properties of Single-Crystalline Co Doped NaFeAs. *New Journal of Physics*, **14**, Article ID: 113043. https://doi.org/10.1088/1367-2630/14/11/113043

[14] Igawa, K., Okada, H., Takahashi, H., Matsuishi, S., Kamihara, Y., Hirano, M., Hosono, H., Matsubayashi, K. and Uwatoko, Y. (2009) Pressure-Induced Superconductivity in Iron Pnictide Compound $SrFe_2As_2$. *Journal of the Physical Society of Japan*, **78**, Article ID: 025001. https://doi.org/10.1143/JPSJ.78.025001

[15] Ye, Z.R., Zhang, Y., Xie, B.P. and Feng, D.L. (2013) Angle-Resolved Photoemission Spectroscopy Study on Iron-Based Superconductors. *Chinese Physics B*, **22**, Article ID: 087407. https://doi.org/10.1088/1674-1056/22/8/087407

[16] Laad, M.S. and Craco, L. (2009) Theory of Multiband Superconductivity in Iron Pnictides. *Physical Review Letters*, **103**, Article ID: 017002. https://doi.org/10.1103/PhysRevLett.103.017002

[17] Hu, J., Liu, T. J., Qian, B., Rotaru, A., Spinu, L. and Mao, Z. Q. (2011) Calorimetric Evidence of Strong-Coupling Multiband Superconductivity in $Fe(Te_{0.57}Se_{0.43})$ Single Crystal. *Physical Review B*, **83**, Article ID: 134521. https://doi.org/10.1103/PhysRevB.83.134521

[18] Raimondi, R., Jefferson, J.H. and Feiner, L.F. (1996) Effective Single-Band Models for the High-T_c Cuprates. II. Role of Apical Oxygen. *Physical Review B*, **53**, 8774-8788. https://doi.org/10.1103/PhysRevB.53.8774

[19] Hamad, I.J., Manuel, L.O. and Aligia, A.A. (2018) Generalized One-Band Model Based on Zhang-Rice Singlets for Tetragonal CuO. *Physical Review Letters*, **120**, 177001. https://doi.org/10.1103/PhysRevLett.120.177001

[20] Okazaki, K., Ito, Y., Ota, Y., Kotani, Y., Shimojima, T., Kiss, T., *et al.* (2014) Superconductivity in an Electron Band Just above the Fermi Level: Possible Route to BCS-BEC Superconductivity. *Nature*, **4**, Article No. 4109. https://doi.org/10.1038/srep04109

[21] Nagamatsum, J., Nakagawa, N., Muranaka, T., Zenitani, Y. and Akimitsu, J. (2001) Superconductivity at 39 K in Magnesium Diboride. *Nature*, **410**, 63-64. https://doi.org/10.1038/35065039

[22] Xi, X.X. (2008) Two-Band Superconductor Magnesium Diboride. *Reports on Progress in Physics*, **71**, Article ID: 116501. https://doi.org/10.1088/0034-4885/71/11/116501

[23] Burmistrova, A.V., Devyatov, I.A., Golubov, A.A., Yada, K. and Tanaka, Y. (2013) The Theory of Tunnelling Spectroscopy of Multiband Superconductors. *Journal of the Physical Society of Japan*, **82**, Article ID: 034716.

https://doi.org/10.7566/JPSJ.82.034716

[24] Nomura, T. (2008) Possibility of Unconventional Pairing due to Coulomb Interaction in Fe-Based Pnictide Superconductors: Perturbative Analysis of Multi-Band Hubbard Models. *Journal of the Physical Society of Japan*, **77**, 123-124. https://doi.org/10.1143/JPSJS.77SC.123

[25] Kuchinskii, E.Z. and Sadovskii, M.V. (2010) Multiple Bands: A Key to High Temperature Superconductivity in Iron Arsenides? *Physica C*, **470**, S418-S419. https://doi.org/10.1016/j.physc.2009.08.005

[26] Terashima, K., Sekiba, Y., Bowen, J.H., Nakayama, K., Kawahara, T., Sato, T., *et al*. (2009) Fermi Surface Nesting Induced Strong Pairing in Iron-Based Superconductors. *Proceedings of the National Academy of Sciences of the United States of America*, **106**, 7330-7333. https://doi.org/10.1073/pnas.0900469106

[27] Rani, L. and Ajay (2013) Electronic Spectra of Iron Pnictide Superconductors: Influence of Multiorbitals Hopping and Hund's Coupling. *Journal of Superconductivity and Novel Magnetism*, **26**, 527-538. https://doi.org/10.1007/s10948-012-1780-1

[28] Rani, L. and Ajay (2015) Influence of Multi-Orbital Hopping and Anisotropy in Intra and Interorbital Coulomb Interactions on the Electronic Spectra in Iron Pnictide Superconductors. *Physica C*, **510**, 31-41. https://doi.org/10.1016/j.physc.2015.01.003

[29] Raghu, S., Qi, X.L., Liu, C.X., Scalapino, D.J. and Zhang, S.C. (2008) Minimal Two-Band Model of the Superconducting Iron Oxypnictides. *Physical Review B*, **77**, Article ID: 220503. https://doi.org/10.1103/PhysRevB.77.220503

[30] Han, Q., Chen, Y. and Wang, Z.D. (2008) A Generic Two-Band Model for Unconventional Superconductivity and Spin-Density-Wave Order in Electron- and Hole-Doped Iron-Based Superconductors. *Europhysics Letters*, **82**, Article ID: 37007. https://doi.org/10.1209/0295-5075/82/37007

[31] Nuwal, A., Kakani, S. and Kakani, S.L. (2014) Two Band Model for the Iron Based Superconductors. *Indian Journal of Pure and Applied Physics*, **52**, 411-422.

[32] Maksimov, E.G., Karakozov, A.E., Gorshunov, B.P., Prokhorov, A.S., Voronkov, A.A., Zhukova, E.S., *et al*. (2011) Two-Band Bardeen-Cooper-Schrieffer Superconducting State of the Iron Pnictide Compound $Ba(Fe_{0.9}Co_{0.1})_2As_2$. *Physical Review B*, **83**, Article ID: 140502. https://doi.org/10.1103/PhysRevB.83.140502

[33] Nuwal, A., Kakani, S. and Kakani, S.L. (2014) Generalized Multiple Gap Model for the Superconductivity in Fe-As Based Superconductors. *SOP Transactions on theoretical Physics*, **1**, 7-26. https://doi.org/10.15764/TPHY.2014.02002

[34] Daghofer, M., Nicholson, A., Moreao, A. and Dagotto, E. (2010) Three Orbital Model for the Iron Based Superconductors. *Physical Review B*, **81**, Article ID: 014511. https://doi.org/10.1103/PhysRevB.81.014511

[35] Ummarino, G.A., Tortello, M., Daghero, D. and Gonnelli, R.S. (2009) Three-Band $s\pm$ Eliashberg Theory and the Superconducting Gaps of Iron Pnictides. *Physical Review B*, **80**, Article ID: 172503. https://doi.org/10.1103/PhysRevB.80.172503

[36] Mockli, D. and de Mello, E.V.L. (2015) Effective Three Band Structure in Fe Based Superconductors. *Europhysics Letters*, **109**, Article ID: 17011. https://doi.org/10.1209/0295-5075/109/17011

[37] Khandka, S. and Singh, P. (2007) Effect of Interlayer Interaction on Tc with Number of Layers in high Tc Cuprate Superconductors. *Physica Status Solidi* (*B*), **244**, 699-708. https://doi.org/10.1002/pssb.200542285

[38] Mukubwa, A. (2018) Electronic Specific Heat of Iron Pnictides Based on Electron-Cooper Pair Interaction. *Open Access Library Journal*, **5**, Article No. e5107.

https://doi.org/10.4236/oalib.1105107

[39] Ahmed Mohamed, E., Ali Ahmed, N., Babiker Hussein, M., Mohammad Taha, R., Ahmed, M. and Abd-Alla, M. (2020) Explanation of Pressure Effect for High Temperature Superconductors Using Pressure Dependent Schrodinger Equation and String Theory. *Natural Science*, **12**, 28-34. https://doi.org/10.4236/ns.2020.121004

[40] Zhigadlo, N.D., Weyeneth, S., Katrych, S., Moll, P.J.W., Rogacki, K., Bosma, S., Puzniak, R., Karpinski, J. and Batlogg, B. (2012) High-Pressure Flux Growth, Structural, and Superconducting Properties of LnFeAsO (Ln = Pr, Nd, Sm) Single Crystals. *Physical Review B*, **86**, Article ID: 214509.

[41] Chen, T.Y., Tesanovic, Z., Liu, R.H., Chen, X.H. and Chien, C.L. (2008) A BCS-Like Gap in the Superconductor $SmFeAsO_{0.85}F_{0.15}$. *Nature*, **453**, 1224-1227. https://doi.org/10.1038/nature07081

[42] Orozco, S., Ortiz, M.A., Moreno, M.R.M. and Murguıa, G. (2012) A Multiband Model for $SmFeAsO_{1-x}F_x$. *Journal of Physics*: *Conference Series*, **400**, Article ID: 022094. https://doi.org/10.1088/1742-6596/400/2/022094

[43] Ryan, D.H., Cadogan, J.M., Ritter, C., Canepa, F., Palenzona, A. and Putti, M. (2009) Coexistence of Long-Ranged Magnetic Order and Superconductivity in the Pnictide Superconductor $SmFeAsO_{1-x}F_x$ (x = 0,0.15). *Physical Review B*, **80**, Article ID: 220503. https://doi.org/10.1103/PhysRevB.80.220503

[44] Johnston, D.C. (2010) The Puzzle of High Temperature Superconductivity in Layered Iron Pnictides and Chalcogenides. *Advances in Physics*, **59**, 803-1061. https://doi.org/10.1080/00018732.2010.513480

[45] Ding, L., He, C., Dong, J.K., Wu, T., Liu, R.H., Chen, X.H. and Li, S.Y. (2008) Specific Heat of the Iron-Based High-T_c Superconductor $SmO_{1-x}F_xFeAs$. *Physical Review B*, **77**, Article ID: 180510. https://doi.org/10.1103/PhysRevB.77.180510

[46] Oh, H., Moon, J., Shin, D., Moon, C.-Y. and Choi, H.J. (2011) Brief Review on Iron-Based Superconductors: Are There Clues for Unconventional Superconductivity? *Progress in Superconductivity*, **13**, 65-84.

[47] Mazin, I.I., Singh, D.J., Johannes, M.D. and Du, M.H. (2008) Unconventional Superconductivity with a Sign Reversal in the Order Parameter of $LaFeAsO_{1-x}F_x$. *Physical Review Letters*, **101**, Article ID: 057003. https://doi.org/10.1103/PhysRevLett.101.057003

[48] Chen, W.Q., Yang, K.V., Zhou, Y. and Zhang, F.C. (2009) Strong Coupling Theory for Superconducting Iron Pnictides. *Physical Review Letters*, **102**, Article ID: 047006. https://doi.org/10.1103/PhysRevLett.102.047006

[49] Zhang, J., Sknepnek, R., Fernandes, R.M. and Schmalian, J. (2009) Orbital Coupling and Superconductivity in the Iron Pnictides. *Physical Review B*, **79**, Article ID: 220502. https://doi.org/10.1103/PhysRevB.79.220502

[50] Nandi, S., Su, Y., Xiao, Y., Price, S., Wang, X.F., Chen, X.H., *et al*. (2011) Strong Coupling of Sm and Fe Magnetism in SmFeAsO as Revealed by Magnetic X-Ray Scattering. *Physical Review B*, **84**, Article ID: 054419. https://doi.org/10.1103/PhysRevB.84.054419